Hindawi
Wireless Communications and Mobile Computing
Volume 2022, Article ID 9901960, 10 pages
https://doi.org/10.1155/2022/9901960

Research Article

AI-Empowered Propagation Prediction and Optimization for Reconfigurable Wireless Networks

Fusheng Zhu,[1] **Weiwen Cai**,[2] **Zhigang Wang**,[1] **and Fang Li**[1]

[1]*Guangdong Communications and Networks Institute, China*
[2]*China Mobile Communications Group Guangdong Co., Ltd., China*

Correspondence should be addressed to Fusheng Zhu; zhufusheng@gdcni.cn

Received 28 September 2021; Accepted 30 November 2021; Published 17 January 2022

Academic Editor: Li Zhu

Vehicular ad-hoc network (VANET) is one of the most important components to realizing intelligent connected vehicles, which is a high-commercial-value vertical application of the fifth-generation (5G) mobile communication system and beyond communications. VANET requires both ultrareliable low latency and high-data rate communications. In order to evolve towards the reconfigurable wireless networks (RWNs), the 5G mobile communication system is expected to adapt the key parameters of its radio nodes rapidly. However, the current propagation prediction approaches are difficult to balance accuracy and efficiency, which makes the current network unable to perform autonomous optimization agilely. In order to break through this bottleneck, an accurate and efficient propagation prediction and optimization method empowered by artificial intelligence (AI) is proposed in this paper. Initially, a path loss model based on a multilayer perception neural network is established at 2.6 GHz for three base stations in an urban environment. Not like empirical models using environment types or deterministic models employing three-dimensional environment models, this AI-empowered model explores the environment feature by introducing interference clutters. This critical innovation makes the proposed model so accurate as ray tracing but much more efficient. Then, this validated model is utilized to realize a coverage prediction for 20 base stations only within 1 minute. Afterward, key parameters of these base stations, such as transmission power, elevation, and azimuth angles of antennas, are optimized using simulated annealing. This whole methodology paves the way for evolving the current 5G network to RWNs.

1. Introduction

With the gradual deepening of global urbanization and industrialization, intelligent transportation systems (ITS) are developing rapidly. For railway transportation, communication-based train control (CBTC) systems are the burgeoning directions for developing future train control systems [1–3]. In vehicular ad-hoc network (VANET), there are four architectures: vehicle-to-vehicle (V2V), vehicle-to-infrastructure (V2I), vehicle-to-pedestrians (V2P), and vehicle-to-anything (V2X). VANET is one of the most important component to realizing intelligent connected vehicles, which is high-commercial-value vertical application of the fifth-generation (5G) mobile communication system and beyond communications. Driven by the emergence of sophisticated and ubiquitous applications and the ever-growing need for information (anytime, anywhere), wireless networks are evolving into profoundly more complex and dynamic systems—reconfigurable wireless networks (RWNs) [4]. Such an intelligent and software-defined design paradigm is the evolution direction of the current 5G mobile communication system as well as one of the keys enabling technologies of sixth-generation (6G) [5, 6]. A comprehensive overview of RWNs and an in-depth analysis of reconfiguration at all layers of the protocol stack are presented in [4], from which it can be seen that the reconfiguration at the PHY layer covers a broad range of topics such as adaptive modulation, antenna beamforming, and software-defined radio (SDR). A good example of reconfiguration is that the current 5G radio nodes, e.g., a NodeB, can support various multiple-in multiple-out (MIMO) options. In principle, the 5G base stations already possess the ability to reconfigure

and adapt their hardware and software components for better coverage and lower interference. As shown in Figure 1, as an example, it will be practically valuable if the key parameters of base stations, such as elevation and azimuth angles of an antenna, transmission power, etc., can be adapted agilely. However, the bottleneck of realizing this reconfiguration is that the propagation prediction models must be both accurate and efficient [7, 8].

In general, propagation models fall into three categories, empirical models, deterministic models, and hybrid models.

(i) Empirical models are based on extensive propagation measurements in various environments at different frequency bands. The typical example is that the path loss models in 3GPP 38.901 are mainly empirically established [9, 10]. Since the generalization ability of empirical models is relatively limited, studies have to be made for each of the specific environment types for different use cases. For instance, there have been many studies on sub-6 GHz channels or mmWave bands in various railway environments [11, 12], such as tunnel [13, 14], plain [15], viaduct [16], cutting [17, 18], crossing bridge [19], and train station [20, 21]. Propagation measurements and empirical studies can be found in more special environments, such as onboard cars [22, 23], aircraft [24, 25], ships [26], and containers [27]

(ii) Deterministic models are based on electromagnetic (EM) calculation (like full-wave solutions such as the method of moments (MoM) [28], finite element method (FEM), and finite-difference time domain (FDTD) [29]), and therefore, they are more accurate than empirical models but much more time-consuming. A typical deterministic model used for coverage prediction is ray tracing (RT), which is a high-frequency approximation technique [30]. Its applications can be found from sub-6 GHz to terahertz (THz), and from narrowband to ultrabroadband in various environments with approved accuracy [31–35]. However, even though the RT simulator can be deployed on high-performance computing (HPC) clusters, like CloudRT (http://www.raytracer.cloud)—an open access HPC RT platform [36]—the computational efficiency is still not comparable with empirical models. Moreover, the highly accurate three-dimensional (3D) environment models are mandatary for RT simulations. Thus, there is still a long way to go before applying deterministic models for rapid network optimization

(iii) Hybrid models usually take advantage of both sides. For instance, a hybrid ray and graph channel model is proposed in [37] to effectively model the diffuse scattering components by adding scattered points around principle paths traced by RT. The authors of [38] provided an overview of map-based mmWave channel models and guidelines of the categorization of map-based channel parameters that possess the following: the map-based deterministic channel parameter, the map-based stochastic channel parameter, and the map-based hybrid channel parameter. Hybrid models are with lower complexity compared to deterministic models, but still, the 3D environment models with not only geometrical information but also material EM properties are required

To summarize, classic propagation models discussed above are not able to balance accuracy and efficiency, either describing the propagation environment qualitatively like urban, suburban, etc. for empirical models or requiring very accurate 3D environment models with geometrical and EM information of material, which in reality not even most areas can support. Thus, the lack of an accurate and efficient propagation prediction model is already the bottleneck for wireless networks to perform autonomous optimization agilely. Recently, there has been a new trend to apply big data analytics to wireless channel modeling [39]. Several studies emerged to investigate various applications of big data analytics, especially machine learning algorithms in wireless communications and channel modeling. For instance, the authors of [40] proposed big data and machine learning-enabled wireless channel model framework. The proposed channel model is based on artificial neural networks (ANNs), including feed-forward neural network (FNN) and radial basis function neural network (RBF-NN). The authors of [41] presented a machine learning approach for the extraction of radio wave propagation models in tunnels. In [42], the authors developed a channel state information (CSI) extraction tool and investigated the performance of channel prediction with a deep learning approach and an autoregression (AR) approach based on realistic measurement data in vehicular environments. The authors of [43] proposed a machine learning-based method for the calibration of stochastic radio propagation models. In [44], the authors proposed prediction methods for path loss and delay spread in air-to-ground mmWave channels based on machine learning. These studies improved channel modeling by taking advantage of the strong ability of artificial intelligence (AI) to express nonlinear relationships and inspired our study in this paper.

In order to break through the bottleneck of realizing an agile network optimization for evolving the current 5G network to future RWNs, a methodology of AI-empowered propagation prediction and optimization is prepared in this paper with the following contributions:

(i) A path loss model based on a multilayer perception (MLP) neural network is established at 2.6 GHz for three base stations in a typical urban environment. Not like empirical models using environment types or deterministic models employing 3D environment models, this AI-empowered model explores the environment feature by introducing interference clutters. This critical innovation makes the proposed model so accurate as RT to have the mean

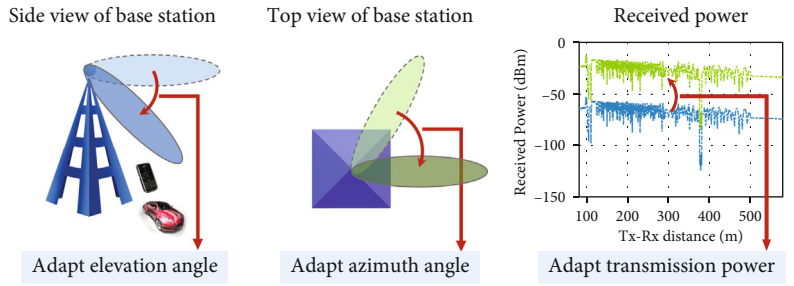

Figure 1: Key parameters of base stations that should be able to adapt agilely in RWNs.

error (ME) of 0.23 dB and the standard deviation (Std) of 4.10 dB

(ii) We provide a case study of using the proposed MLP neural network to realize a coverage prediction for 20 base stations in an urban area. The whole prediction can be completed within 1 minute, implying a considerable improvement in simulation efficiency compared to RT. Moreover, the proposed MLP neural network does not require a 3D environment model. This makes the model much easier to be used in practice

(iii) Based on predicted coverage, an autonomous optimization method enabled by simulated annealing is proposed to rapidly adapt key parameters of base stations, such as transmission power, elevation, and azimuth angles of antennas. This will then trigger another new round of prediction and optimization

With the contribution mentioned above, the whole methodology gives the 5G radio nodes the ability of autonomous optimization under dynamic conditions, and therefore, paves the way for evolving the current 5G network to RWNs. The rest of this paper is organized as follows: Section 2 describes the whole workflow with the highlight of the novel way of characterizing propagation environment—interference clutters. Based on this new concept, an MLP neural network is established and utilized to predict the coverage of a number of base stations in a given urban area. With the aid of simulated annealing, an autonomous optimization method is proposed in Section 3 to adapt key parameters of base stations for continuous iteration of agile network optimization. Finally, we draw the conclusions in Section 4.

2. Novel Way of Characterizing Propagation Environment

2.1. Workflow Overview. Figure 2 shows the workflow of this paper. In order to avoid complex three-dimensional (3D) scenario modeling, a simple scenario characterization method based on the clutter map is proposed, and a dataset is constructed by combining the environmental features extracted from the clutter map and the cell parameters obtained by measurement. Based on the strong learning ability of artificial intelligence (AI), the multilayer perceptron (MLP) artificial neural network (ANN) is selected to establish the channel prediction model by training the above datasets. Reference signal received power (RSRP) obtained by the AI-based channel modeling can be employed to calculate the coverage and signal to interference plus noise ratio (SINR). Based on the coverage, SINR, and given judgment conditions, the best cell parameters and optimization report can be obtained.

2.2. Characterizing Environmental Features. Obstacles are the most important components of the physical environment for radio propagation. For the large-scale complex environment, the complexity of three-dimensional (3D) environment modeling and the diversity of materials on the surface of objects in the environment both seriously affect the accuracy and efficiency of channel modeling. Therefore, this section proposes to employ the limited clutter types to characterize the propagation environment, avoiding the 3D environment modeling, and improving the efficiency of channel modeling.

The electromagnetic (EM) characteristics of materials on the surface of the structures in the environment are important factors affecting the radio propagation. The EM characteristics of materials on the surface of the different clutter types are different. Compared with the accurate environmental information, the distribution of clutter types in the environment can represent the environment to a certain extent.

Using the measurement and electronic map, the 3D spatial position information of any Rx and associated BS can be obtained, as well as the environment type of the measurement scenario. Meanwhile, a straight line L can be uniquely determined by the "BS-Rx" position points. According to the length of the straight line L which passes through each clutter type, the environmental characteristics of the group of measured data can be defined as F_{clutter}, to characterize the radio propagation environment. F_{clutter} can be expressed as

$$F_{\text{clutter}} = (l_1, l_2, \cdots, l_N), \tag{1}$$

where l_i is the length of the straight line L that passes through the ith clutter type, N represents the number of clutter types in the measurement scenario.

2.3. Cell Parameters. Cell parameters are important factors for network optimization. The correctness of cell parameters is related to the accuracy of channel modeling results. In this

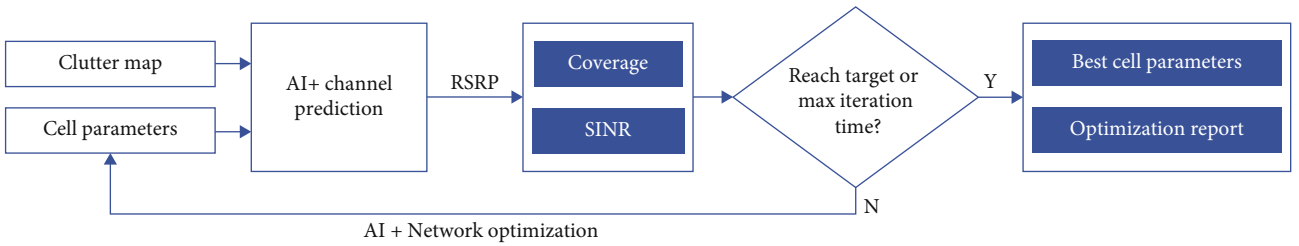

Figure 2: Workflow of AI-empowered propagation prediction and optimization for RWNs.

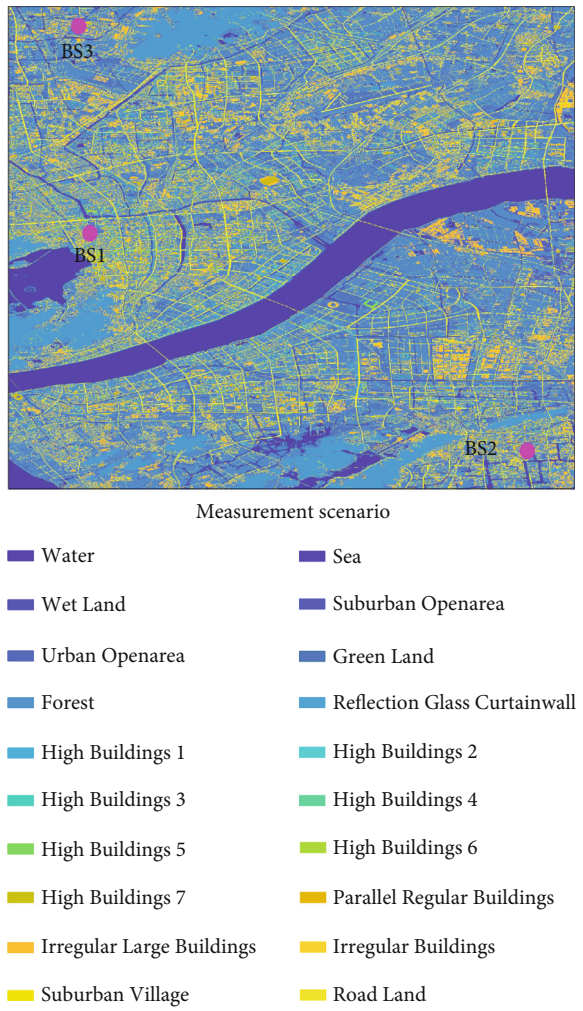

(a) Measurement scenario

(b) Measurement trajectory

Figure 3: Measurement scenario and trajectory.

Table 1: Measurement setups.

Frequency	$F_r = 2.5$ GHz (5G commercial-use license band of China mobile)	
BS	3D location	$L_{BS} = (x_{BS}, y_{BS}, z_{BS})$
	Power	8
	Antenna	Omnidirectional antenna Maximum antenna gain: 4 dBi
	Height	BS1: $H = 62$ m BS2: $H = 30$ m BS3: $H = 41.7$ m
Rx	3D location	$L_{Rx} = (x_{Rx}, y_{Rx}, z_{Rx})$
	Antenna	Omnidirectional antenna Antenna gain: 0 dBi
	Height	$H = 1.5$ m

paper, the measurement method is used to collect cell parameters. As shown in Figure 3, the channel measurement campaign is carried out in different regions of Hangzhou, China. Figure 3(a) shows the digital map of the measured scenario. In this scenario, base stations (BSs) are deployed at three locations, and the receiver (Rx) is deployed on a car with a height of approximately 1.5 m. The trajectory of the car is shown as the red line in Figure 3(b). Detailed measurement setup is shown in Table 1. Measurements are carried out around three BS, and the received power is collected at 23892 different locations (BS1: 10184 groups, BS2: 9988 groups, BS3: 3720 groups).

Path loss (PL) is an important parameter in wireless channel modeling, which represents the reduction of power density in the process of radio propagation and reflects the radio propagation characteristics and channel characteristics. Combined with the measurement setup, the PL corresponding to the measured data can be obtained from the following formula:

$$\mathrm{PL} = P_{Tx} + G_{\mathrm{BS}} + G_{Rx} - P_{Rx}, \tag{2}$$

where PL is the abbreviation for path loss; P_{Tx} represents the emission power; G_{BS} and G_{Rx} represent the antenna gain of BS and Rx, respectively; P_{Rx} is the received power.

2.4. Coverage Ratio. A region to be predicted is divided into mesh grids, and the center of a grid is considered as valid Rx positions according to predefined rules, e.g., outdoor, indoor, or hybrid. A grid is covered if its RSRP is larger than a certain level. In this work, g_i is under good coverage condition when $P_i > -90$ dBm. Therefore, we have a coverage ratio of C_r expressed as the number of grids G_c under good coverage condition divided by the total number of valid grids G_v.

2.5. Signal to Interference plus Noise Ratio. The signal to interference plus noise ratio (SINR) of grid i, denoted as g_i, is defined as the power of a certain signal of interest, denoted as P_i, divided by the sum of the interference power, i.e., I, from all the other interfering signals, and the power of some background noise, i.e., noise. The form of SINR can be explicitly written as

$$\mathrm{SINR}(g_i) = \frac{P_i}{(I + \mathrm{Noise})}. \tag{3}$$

In this work, the maximum RSRP is considered as P_i of g_i, Noise = −120 dBm for all Rxs. g_i under good SINR condition when $\mathrm{SINR}(g_i) > 10$ dB. We have SINR S_r expressed as the number of grids under good SINR conditions divided by the total number of valid grids G_v.

2.6. MLP-Based Path Loss Model. An MLP neural network is composed of an input layer, an output layer, and multiple hidden layers and is a multilayer forward neural network trained by back-propagation (BP) algorithm. Compared with other neural networks, MLP neural networks have the advantages of simple structure, easy implementation, good fault tolerance, and strong robustness. Therefore, a PL model is established based on the MLP neural network, its performance is evaluated, this section uses the MLP network to establish a PL model, and its performance is evaluated.

(1) *Preliminary Preparation of Dataset.* ANN is a kind of data-driven mathematical model, and whether the dataset is appropriate or not directly affects the predicted results. The relative position of BS and Rx, the distance between them, and the environment in which they are located are the key factors that affect radio propagation. In this work, the dataset of the MLP neural network is constructed by the measured data and the information of the radio propagation scenario, including the relative position of BS and Rx, the distance between them, and the environmental features extracted from the clutter map. The training data and the test data are randomly selected from the dataset. The number of samples in the training dataset accounts for 70% of the total number of samples. We expect to predict the PL of radio propagation, then the target set of the dataset, that is, the expected output of the MLP neural network, is PL

(2) *Establishment of Path Loss Model.* For the PL model based on the MLP neural network, the selection of the number of neurons directly affects the prediction performance. If the number of neurons is too small, the neural network does not have the necessary learning ability and information processing ability. Conversely, if the network structure is too complex, it will lead to the low efficiency of network learning and prone to overfitting, which will reduce the generalization ability of the PL model

There is no clear theory and method on how to determine the number of neurons. Generally, the number of

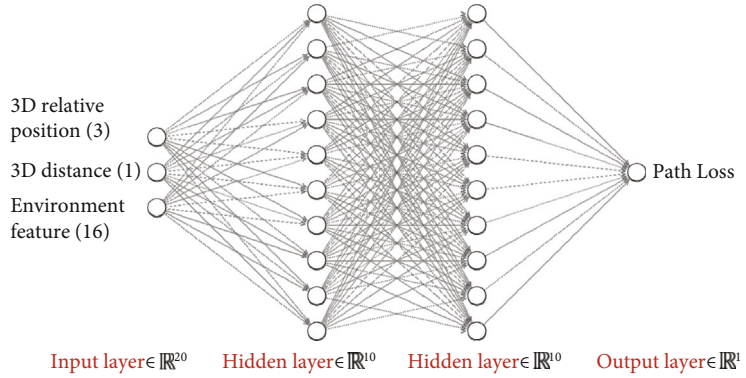

Figure 4: MLP neural network architecture.

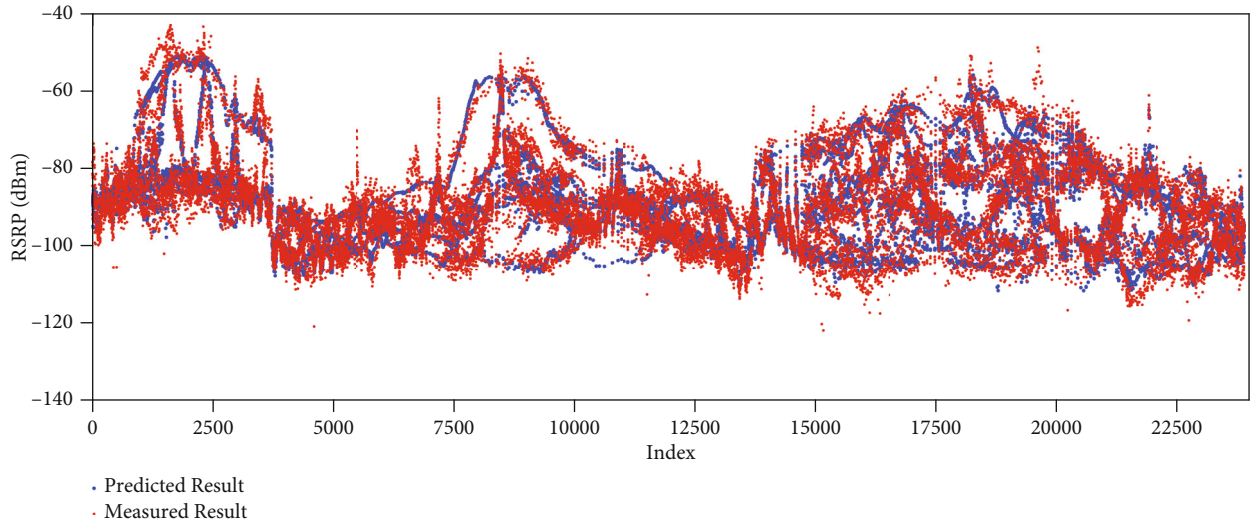

Figure 5: Comparison between the predicted result and the measured result, given ME = 0.23 dB, Std = 4.10 dB.

neurons in ANN can be determined by the following two empirical formulas:

$$N_H = \sqrt{N_I + N_O} + \alpha, \tag{4}$$

$$N_H = \frac{N_{\text{training}}}{\alpha \bullet (N_I + N_O)}, \tag{5}$$

where N_H is the number of neurons in the hidden layer; N_I and N_O are the number of neurons in the input and output layers, respectively; α is a random integer in the range of 1-10; N_{training} is the number of training samples.

After several trials, we find that best and optimal solution is a network architecture with two hidden layers and ten neurons in each hidden layer. As shown in Figure 4, based on the formula (4) and the dimensions of the above dataset, a network architecture with two hidden layers and ten neurons in each hidden layer is finally selected to establish the PL model. Other hyperparameters of this MLP neural network are set as follows: the learning rate is 0.1, the optimizer is adaptive moment estimation (Adam), training times, i.e., E_{poch} is 10000.

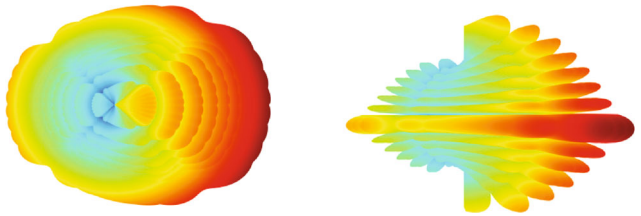

Figure 6: 3D antenna pattern of all BSs.

2.7. Performance Evaluation

(1) *Accuracy*. In this paper, the mean error (ME), the standard deviation (STD) of error, and the correlation coefficient (Corr) between the predicted results and the measured results are employed as the

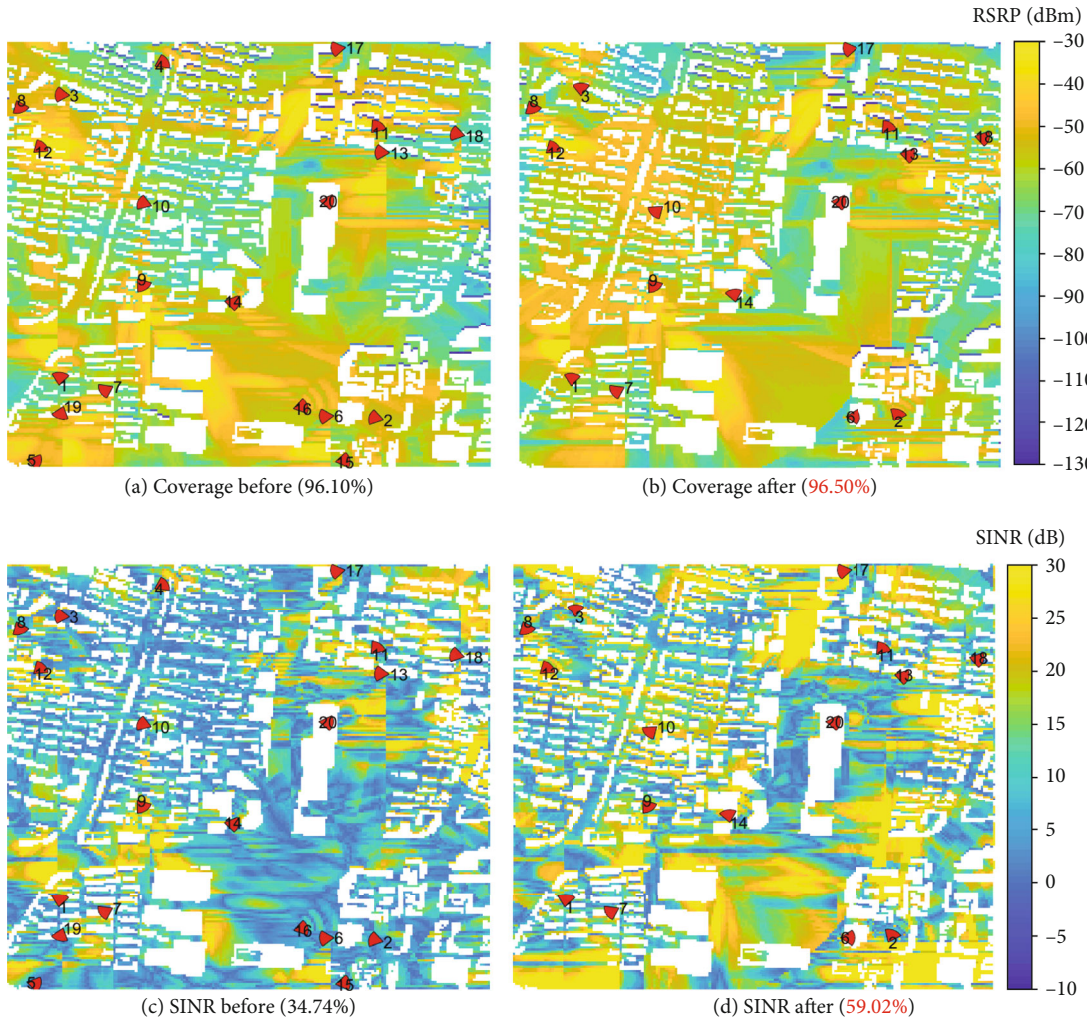

(a) Coverage before (96.10%)

(b) Coverage after (96.50%)

(c) SINR before (34.74%)

(d) SINR after (59.02%)

Figure 7: Coverage and SINR before and after optimization.

indicators to evaluate the performance of the MLP based PL model. Their expressions are as follows:

$$\mathrm{ME} = \frac{\left|\sum_{i=1}^{N_{\mathrm{sample}}} (PL_i + pl_i)\right|}{N_{\mathrm{sample}}}, \tag{6}$$

$$\mathrm{STD} = \sqrt{\frac{\left|\sum_{i=1}^{N_{\mathrm{sample}}} [(PL_i - pl_i) - \mu_{\mathrm{error}}]^2\right|}{N_{\mathrm{sample}}}}, \tag{7}$$

$$Corr = \frac{\sum_{i=1}^{N_{\mathrm{sample}}} (PL_i - \mu_{PL})\left(pl_i - \mu_{pl}\right)}{\sqrt{\sum_{i=1}^{N_{\mathrm{sample}}} (PL_i - \mu_{PL})^2 \left(pl_i - \mu_{pl}\right)^2}}, \tag{8}$$

where pl is the predicted value of PL, N_{sample} is the number of predicted samples. μ_{PL}, μ_{pl}, and μ_{error} are the mean value of PL measured results, the mean value of PL predicted results, and the mean error of PL measured and predicted results, respectively.

The ME and the STD of error are commonly used to measure prediction accuracy. The correlation coefficient is used to evaluate the linear correlation between the predicted and measured results. The closer the predicted results are to the measured results, the greater the correlation between them, and the closer the correlation coefficient is to 1. On the contrary, if there is a great difference between the predicted results and the measured results, the correlation between them is low, and the correlation coefficient tends to 0.

Figure 5 shows the analysis of the error between the measured results PL and the predicted values PL′ of MLP based PL prediction models. The ME and STD of PL prediction models are 0.23 dB and 4.10 dB, respectively. The correlation coefficient between the measured and predicted results is 0.94, which is greater than 0.8. These results show that the prediction model based on MLP can predict PL more accurately.

Table 2: The optimization outcomes on SINR and coverage ratio.

Parameter	SINR	Coverage ratio
Before optimization	34.74%	96.10%
After optimization	59.02%	96.50%
Optimization outcomes	24.28%	0.4%

(2) *Case Study of Agile Coverage Prediction*. Based on the validated path loss model, it can be used in the environment is similar features. A 1 km-by-1 km region centered at BS1 is selected to realize coverage prediction. 20 base stations are dropped with random initial parameters; the coverage radius is 1 km for all the BSs. The resolution of the grid is 5 m to be inconsistent with the clutter map of the environment. Therefore, there are 40000 grids within the prediction radius of each BS. As the path loss model is trained for the outdoor environment, the valid grids are located outdoor only. Figure 6 shows the 3D radiation pattern of the antenna for all the base stations; the maximum antenna gain is 17 dBi. The coverage ratio and SINR are obtained efficiently within 1 second. Figures 7(a) and 7(c) show the predicted coverage and SINR, respectively

3. Autonomous Optimization with the Aid of Simulated Annealing

In this work, a simulated annealing method is employed to enable autonomous optimization to maximize coverage ratio and SINR. The key parameters of base stations (including the transmission power, elevation, and azimuth angles of antennas) are adapted iteratively to reduce the cost function:

$$\text{Cost} = 1 - Cr + 1 - Sr. \tag{9}$$

With less than 1000 iteration within 1 minute, the three parameters of the 20 base stations are tuned, and the optimized coverage and SINR are compared in Figure 7. The optimization report indicates that, by changing the directions of some base stations, both coverage ratio and SINR can be increased; some base stations are too close to each other, and rotating antenna direction does not help decrease interference. The algorithm reduces the transmitting power of several base stations to very small, e.g., BS1, 4, 15, 16, 19 should be shut down. In the end, the SINR increases 24.28% with a slightly better coverage ratio after autonomous optimization. The outcomes before and after autonomous optimization are shown in Table 2.

4. Conclusions

This paper presented a methodology of AI-empowered propagation prediction and optimization for reconfigurable wireless networks. With the aid of the new concept—interference clutters—proposed in this study, we established an MLP neural network for path loss prediction at 2.6 GHz for three base stations in a typical urban environment. Validation by real measurements implies that the proposed model is so accurate as deterministic models (like RT) with the ME of 0.23 dB and the Std of 4.10 dB, even without the support of the 3D environment model. Then, a case study of employing this AI-empowered model is to realize a coverage prediction for 20 base stations. The whole prediction can be completed within 1 minute, implying that the proposed model balances accuracy and efficiency very well and even does not require detailed information on propagation environments. This feature improves its practical value in real network optimization. Finally, with the aid of simulated annealing, we presented an autonomous optimization method to rapidly adapt key parameters of base stations, such as transmission power, elevation, and azimuth angles of antennas. In the future, we will further study and discuss more degrees of freedom for network optimization, such as beamwidth. The whole methodology, including prediction and optimization enabled by AI, breakthroughs the bottleneck of realizing an agile network optimization, supports the design of the VANET, and therefore forms the fundamental for evolving the current 5G network to B5G and 6G.

Data Availability

The [DATA TYPE] data used to support the findings of this study are included within the article.

Conflicts of Interest

The authors declare that there is no conflict of interest regarding the publication of this paper.

Acknowledgments

This work was supported by the Key-Area Research and Development Program of Guangdong Province (2020B0101120003).

References

[1] L. Zhu, H. Liang, H. Wang, B. Ning, and T. Tang, "Joint security and train control design in blockchain empowered CBTC system," *IEEE Internet of Things Journal*, 2021.

[2] L. Zhu, Y. Li, F. R. Yu, B. Ning, T. Tang, and X. Wang, "Cross-layer defense methods for jamming-resistant CBTC systems," *IEEE Transactions on Intelligent Transportation Systems*, vol. 22, no. 11, pp. 7266–7278, 2021.

[3] Y. Li, L. Zhu, H. Wang, F. R. Yu, and S. Liu, "A cross-layer defense scheme for edge intelligence-enabled CBTC systems against MitM attacks," *IEEE Transactions on Intelligent Transportation Systems*, vol. 22, no. 4, pp. 2286–2298, 2021.

[4] A. El-Mougy, M. Ibnkahla, G. Hattab, and W. Ejaz, "Reconfigurable wireless networks," *Proceedings of the IEEE*, vol. 103, no. 7, pp. 1125–1158, 2015.

[5] S. Dang, O. Amin, B. Shihada, and M.-S. Alouini, "What should 6G be?," *Nature Electronics*, vol. 3, no. 1, pp. 20–29, 2020.

[6] I. F. Akyildiz, A. Kak, and S. Nie, "6G and beyond: the future of wireless communications systems," *IEEE Access*, vol. 8, pp. 133995–134030, 2020.

[7] T. Wei, W. Feng, N. Ge, and J. Lu, "Environment-aware coverage optimization for space-ground integrated maritime communications," *IEEE Access*, vol. 8, pp. 89205–89214, 2020.

[8] C. Wang, M. D. Renzo, S. Stanczak, S. Wang, and E. G. Larsson, "Artificial intelligence enabled wireless networking for 5G and beyond: recent advances and future challenges," *IEEE Wireless Communications*, vol. 27, no. 1, pp. 16–23, 2020.

[9] U. Karabulut, A. Awada, I. Viering, M. Simsek, and G. P. Fettweis, "Spatial and temporal channel characteristics of 5G 3D channel model with beamforming for user mobility investigations," *IEEE Communications Magazine*, vol. 56, no. 12, pp. 38–45, 2018.

[10] X. Cheng, B. Yu, L. Yang et al., "Communicating in the real world: 3D MIMO," *IEEE Wireless Communications*, vol. 21, no. 4, pp. 136–144, 2014.

[11] J. Moreno, J. Riera, L. De Haro, and C. Rodriguez, "A survey on future railway radio communications services: challenges and opportunities," *IEEE Communications Magazine*, vol. 53, no. 10, pp. 62–68, 2015.

[12] B. Ai, K. Guan, M. Rupp et al., "Future railway services-oriented mobile communications network," *IEEE Communications Magazine*, vol. 53, no. 10, pp. 78–85, 2015.

[13] A. Hrovat, G. Kandus, and T. Javornik, "A survey of radio propagation modeling for tunnels," *IEEE Communications Surveys & Tutorials*, vol. 16, no. 2, pp. 658–669, 2014.

[14] Y. Liu, A. Ghazal, C.-X. Wang, X. Ge, Y. Yang, and Y. Zhang, "Channel measurements and models for high-speed train wireless communication systems in tunnel scenarios: a survey," *Science China Information Sciences*, vol. 60, no. 10, 2017.

[15] C. Wang, J. Bian, J. Sun, W. Zhang, and M. Zhang, "A survey of 5G channel measurements and models," *IEEE Communications Surveys Tutorials*, vol. 20, no. 4, pp. 3142–3168, 2018.

[16] X. Yin, X. Cai, X. Cheng, J. Chen, and M. Tian, "Empirical geometry- based random-cluster model for high-speed-train channels in UMTS networks," *IEEE Transactions on Intelligent Transportation Systems*, vol. 16, no. 5, pp. 2850–2861, 2015.

[17] D. He, B. Ai, K. Guan et al., "Influence of typical railway objects in a mmWave propagation channel," *IEEE Transactions on Vehicular Technology*, vol. 67, no. 4, pp. 2880–2892, 2018.

[18] J. Yang, B. Ai, K. Guan et al., "A geometry-based stochastic channel model for the millimeter-wave band in a 3GPP high-speed train scenario," *IEEE Transactions on Vehicular Technology*, vol. 67, no. 5, pp. 3853–3865, 2017.

[19] K. Guan, Z. Zhong, B. Ai, and T. Kurner, "Propagation measurements and modeling of crossing bridges on high-speed railway at 930 MHz," *IEEE Transactions on Vehicular Technology*, vol. 63, no. 2, pp. 502–517, 2014.

[20] K. Guan, Z. Zhong, B. Ai, and T. Kurner, "Empirical models for extra propagation loss of train stations on high-speed railway," *IEEE Transactions on Antennas and Propagation*, vol. 62, no. 3, pp. 1395–1408, 2014.

[21] J. Lee, J. Liang, M.-D. Kim, J. J. Park, B. Park, and H. K. Chung, "Measurement-based propagation channel characteristics for millimeter-wave 5G giga communication systems," *ETRI Journal*, vol. 38, no. 6, pp. 1031–1041, 2016.

[22] C. U. Bas and S. C. Ergen, "Ultra-wideband channel model for intra-vehicular wireless sensor networks beneath the chassis: from statistical model to simulations," *IEEE Transactions on Vehicular Technology*, vol. 62, no. 1, pp. 14–25, 2013.

[23] L. Cheng, J. Casazza, J. Grace, F. Bai, and D. D. Stancil, "Channel propagation measurement and modeling for vehicular in-cabin Wi-Fi networks," *IEEE Transactions on Antennas and Propagation*, vol. 64, no. 12, pp. 5424–5435, 2016.

[24] R. D'Errico and L. Rudant, "UHF radio channel characterization for wireless sensor networks within an aircraft," in *Proceedings of the 5th European Conference on Antennas and Propagation (EUCAP)*, pp. 115–119, Rome, Italy, 2011.

[25] H. Saghir, C. Nerguizian, J. J. Laurin, and F. Moupfouma, "In-cabin wideband channel characterization for WAIC systems," *IEEE Transactions on Aerospace and Electronic Systems*, vol. 50, no. 1, pp. 516–529, 2014.

[26] X. H. Mao and Y. H. Lee, "UHF propagation along a cargo hold on board a merchant ship," *IEEE Transactions on Wireless Communications*, vol. 12, no. 1, pp. 22–30, 2013.

[27] E. Tanghe, W. Joseph, P. Ruckebusch, L. Martens, and I. Moerman, "Intra-, inter-, and extra-container path loss for shipping container monitoring systems," *IEEE Antennas and Wireless Propagation Letters*, vol. 11, pp. 889–892, 2012.

[28] R. F. Harrington, *Field Computation by Moment Methods*, Wiley-IEEE Press, 1993.

[29] J. W. Schuster and R. J. Luebbers, "Comparison of GTD and FDTD predictions for UHF radio wave propagation in a simple outdoor urban environment," in *IEEE Antennas and Propagation Society International Symposium 1997. Digest*, vol. 3, pp. 2022–2025, Montreal, QC, Canada, July 1997.

[30] C.-F. Yang, B.-C. Wu, and C.-J. Ko, "A ray-tracing method for modeling indoor wave propagation and penetration," *IEEE Transactions on Antennas and Propagation*, vol. 46, no. 6, pp. 907–919, 1998.

[31] C. Oestges, G. Hennaux, and Q. Gueuning, "Centimeter- and millimeter-wave channel modeling using ray-tracing for 5G communications," in *2015 IEEE 82nd vehicular technology conference (VTC2015-fall)*, pp. 1–5, Boston, MA, USA, 2015.

[32] S. Hur, S. Baek, B. Kim et al., "28 GHz channel modeling using 3D ray-tracing in urban environments," in *2015 9th European Conference on Antennas and Propagation (EuCAP)*, pp. 1–5, Lisbon, Portugal, May 2015.

[33] K. Kimura and J. Horikoshi, "Prediction of wideband propagation characteristics of the millimeter-wave in the mobile radio environment," in *Universal Personal Communications, 1998. ICUPC '98. IEEE 1998 International Conference on, vol. 1*, pp. 3–7, Florence, Italy, October 1998.

[34] B. Ai, K. Guan, R. He et al., "On indoor millimeter wave massive MIMO channels: measurement and simulation," *IEEE Journal on Selected Areas in Communications*, vol. 35, no. 7, pp. 1678–1690, 2017.

[35] S. Priebe and T. Kurner, "Stochastic modeling of THz indoor radio channels," *IEEE Transactions on Wireless Communications*, vol. 12, no. 9, pp. 4445–4455, 2013.

[36] D. He, B. Ai, K. Guan, L. Wang, Z. Zhong, and T. Kurner, "The design and applications of high-performance ray-tracing simulation platform for 5g and beyond wireless communications: a tutorial," *IEEE Communications Surveys Tutorials*, vol. 21, no. 1, pp. 10–27, 2019.

[37] D. He, K. Guan, J. M. García-Loygorri et al., "Channel characterization and hybrid modeling for millimeter-wave communications in metro train," *IEEE Transactions on Vehicular Technology*, vol. 69, pp. 12408–12417, 2020.

[38] Y. G. Lim, Y. J. Cho, M. S. Sim, Y. Kim, C. B. Chae, and R. A. Valenzuela, "Map-based millimeter-wave channel models: an

overview, data for B5G evaluation and machine learning," *IEEE Wireless Communications*, vol. 27, no. 4, pp. 54–62, 2020.

[39] W. H. Chin, Z. Fan, and R. Haines, "Emerging technologies and research challenges for 5G wireless networks," *IEEE Wireless Communications*, vol. 21, no. 2, pp. 106–112, 2014.

[40] J. Huang, C. Wang, L. Bai et al., "A big data enabled channel model for 5G wireless communication systems," *IEEE Transactions on Big Data*, vol. 6, no. 2, pp. 211–222, 2020.

[41] A. Seretis, X. Zhang, K. Zeng, and C. D. Sarris, "Artificial neural network models for radiowave propagation in tunnels," *IET Microwaves, Antennas Propagation*, vol. 14, no. 11, pp. 1198–1208, 2020.

[42] J. Joo, M. C. Park, D. S. Han, and V. Pejovic, "Deep learning-based channel prediction in realistic vehicular communications," *IEEE Access*, vol. 7, pp. 27 846–27 858, 2019.

[43] R. Adeogun, "Calibration of stochastic radio propagation models using machine learning," *IEEE Antennas and Wireless Propagation Letters*, vol. 18, no. 12, pp. 2538–2542, 2019.

[44] G. Yang, Y. Zhang, Z. He, J. Wen, Z. Ji, and Y. Li, "Machine-learning-based prediction methods for path loss and delay spread in air-to-ground millimetre-wave channels," *IET Microwaves, Antennas Propagation*, vol. 13, no. 8, pp. 1113–1121, 2019.